# Neuregulin1 displayed on motor axons regulates terminal Schwann cell-mediated synapse elimination at developing neuromuscular junctions

Young il Lee[a,1], Yue Li[b], Michelle Mikesh[c], Ian Smith[d], Klaus-Armin Nave[e], Markus H. Schwab[f], and Wesley J. Thompson[a,1]

[a]Department of Biology, Texas A&M University, College Station, TX 77843; [b]Dell Pediatric Research Institute, The University of Texas, Austin, TX 78712; [c]Section of Molecular Cell and Developmental Biology, The University of Texas, Austin, TX 78712; [d]Institute for Neuroscience, Texas A&M University, College Station, TX 77843; [e]Department of Neurogenetics, Max Planck Institute of Experimental Medicine, 37075 Göttingen, Germany; and [f]Department of Cellular Neurophysiology, Hannover Medical School, 30625 Hannover, Germany

Synaptic connections in the nervous system are rearranged during development and in adulthood as a feature of growth, plasticity, aging, and disease. Glia are implicated as active participants in these changes. Here we investigated a signal that controls the participation of peripheral glia, the terminal Schwann cells (SCs), at the neuromuscular junction (NMJ) in mice. Transgenic manipulation of the levels of membrane-tethered neuregulin1 (NRG1-III), a potent activator of SCs normally presented on motor axons, alters the rate of loss of motor inputs at NMJs during developmental synapse elimination. In addition, NMJs of adult transgenic mice that expressed excess axonal NRG1-III exhibited continued remodeling, in contrast to the more stable morphologies of controls. In fact, synaptic SCs of these adult mice with NRG1-III overexpression exhibited behaviors evident in wild type neonates during synapse elimination, including an affinity for the postsynaptic myofiber surface and phagocytosis of nerve terminals. Given that levels of NRG1-III expression normally peak during the period of synapse elimination, our findings identify axon-tethered NRG1 as a molecular determinant for SC-driven neuromuscular synaptic plasticity.

synapse elimination | neuromuscular junction | Schwann cell | neuregulin1 | synaptic competition

Synaptic connections found in the mature nervous system differ significantly from those formed during development. This developmental transformation includes elimination and remodeling of existing synapses, commonly termed "synapse elimination," and is seen throughout the nervous system (1, 2). Similar remodeling can occur throughout life during learning, aging, and disease, however (3–5).

The process of synapse elimination has been studied most extensively in rodent neuromuscular junctions (NMJs). At each mature NMJ, high-density aggregates of acetylcholine receptors (AChRs) on the muscle fiber are apposed precisely by the terminal arbor of a motor axon. Processes of nonmyelinating glia—terminal Schwann cells (tSCs)—cap this synaptic structure. These tSCs sense the release of acetylcholine and ATP by the nerve and in turn influence transmitter release (6, 7). During 2–3 wk of postnatal development, pruning of up to ∼10 converging motor axons occurs until one axon remains at each NMJ (8–10). This elimination involves the remodeling of terminal arbors and withdrawal of displaced branches rather than motor neuron death. Vital imaging of developing NMJs has provided compelling evidence that competition among axons determines the sole winner (11, 12). Activity patterns (13, 14) and the relative efficacy of converging presynaptic inputs (15) are factors known to influence the rate of elimination and the winner. Nevertheless, despite these findings, the cellular mechanisms or molecules that govern this process remain largely unknown.

We recently observed novel tSC behaviors at neonatal junctions, with tSCs phagocytosing nerve terminals and competing

with them for contact with the muscle surface (16). These activities appear to drive interterminal competition through random displacement of inputs (11). The occupation of the postsynaptic surface by tSCs also may provide a mechanism by which immature "plaques" of AChR acquire mature, "pretzel"-like configurations (17, 18). AChRs, silenced by tSC interposition between the terminal and muscle, on a still active muscle fiber, would be subject to removal (19). These activities of postnatal tSCs are not present in adults, where the arrangement of all three synaptic components is mostly stable. Molecular signals that promote these differing behaviors of neonatal tSCs remain obscure, however. As noted previously (16, 20), the tSC activities in separating axons from each other and their target muscle fibers resemble SC behaviors during development of the peripheral nerves (21), suggesting possible overlap in the signals.

The *Nrg1* gene, through alternative splicing, codes for a family of neuregulin1 (NRG1) proteins implicated in a number of biological processes (22–24). Type III NRG1 (NRG1-III), a membrane-tethered isoform shown to regulate sorting and myelination of peripheral axons by SCs (25, 26), is the chief splice variant in developing spinal cord, and its expression appears to be highly restricted to motor neurons (27, 28). Whereas early experiments suggested that motor neuron-derived NRG1 stimulates muscle AChR synthesis (29, 30), ensuing gene inactivation studies (31, 32) established that normal NMJs form in the absence of NRG1

**Significance**

Refinement of synaptic connections occurs throughout the nervous system and is essential for its proper function. Significant gaps remain in our understanding of the mechanisms that mediate pruning of synaptic connections—a form of synaptic plasticity known as synapse elimination. Recently it has become clear there is significant glial cell involvement. The present study of the rodent neuromuscular junction addresses two outstanding questions involving this glial involvement: which molecules determine the Schwann cell behavior present during pruning, and whether these behaviors actually alter synaptic structure. Our findings identify axon-tethered neuregulin1 as a molecular determinant for Schwann cell-driven neuromuscular synaptic plasticity.

signaling in myofibers. Here we show that NRG1-III regulates tSC behaviors that promote neuromuscular synaptic plasticity. The rate at which polyneuronal innervation is lost from developing NMJs correlates with the level of axo-glial NRG1-III signaling. Overexpression of NRG1-III in motor axons results in tSCs that maintain a neonatal phenotype into adulthood, leading to continued morphological changes of the synapses. Collectively, these findings suggest that NRG1-III, whose expression peaks early in postnatal development, promotes plasticity of NMJs via its actions on tSCs.

## Results

### NRG1-III Expression Peaks During the Period of Developmental Neuromuscular Synapse Elimination.

SC behaviors during the development of peripheral nerves are regulated by axonal expression of NRG1-III (25, 26). Because these behaviors resemble those of tSCs at neonatal NMJs (16), we hypothesized that axonal NRG1 regulates synapse elimination. This hypothesis is consistent with the observation that NMJs are most sensitive to exogenous NRG during the period of synapse elimination (33). Schwann cells are known to have receptors for NRG1 (34). Moreover, NRG1-III expression in rat brain is reported to peak in early postnatal development, during the period of synapse elimination (35). Therefore, we sought to determine whether NRG1-III expression is regulated in the spinal cord in a manner temporally consistent with synapse elimination.

NRG1-III is the major isoform produced by motor neurons—the cell type responsible for virtually all NRG1-III transcripts found in developing spinal cord (27, 28). We compared the levels of NRG1-III expression in spinal cords of wild type (WT) pups during the first 3 postnatal weeks beginning at birth, as well as at two adult stages, via quantitative real-time PCR (qRT-PCR). NRG1-III transcript levels were highest during the second postnatal week of life and declined as the mice matured (Fig. 1A). At its peak at postnatal day (P) 9, NRG1-III mRNA was approximately eightfold greater than the lowest levels observed at P133 ($P < 0.001$; $n = 3$). These results are thus consistent with the idea that tSC behavior during synapse elimination (16) is a response to the normally elevated NRG1-III levels present on motor axons.

### NRG1-III Signaling Regulates the Rate of Synapse Elimination.

If NRG1-III–regulated tSC behaviors contribute to the removal of redundant inputs at developing NMJs, then changing the strength of NRG1-III signaling should alter the time course of synapse elimination. We first examined neonatal mice in which NRG1-III is overexpressed under control of the thy1.2 promoter (25). This promoter drives transgenic NRG1-III expression, which mimics the endogenous NRG1-III distribution, i.e., motor neurons and dorsal root ganglia (36). Thus, in the context of NMJs, transgenic NRG1-III expression is motor neuron-selective. We detected an increase in NRG1-III transcripts in the spinal cords of transgenic pups by P3, in line with a previous report (37). This overexpression was maintained into adulthood (Fig. 1B). Because NRG1 is a
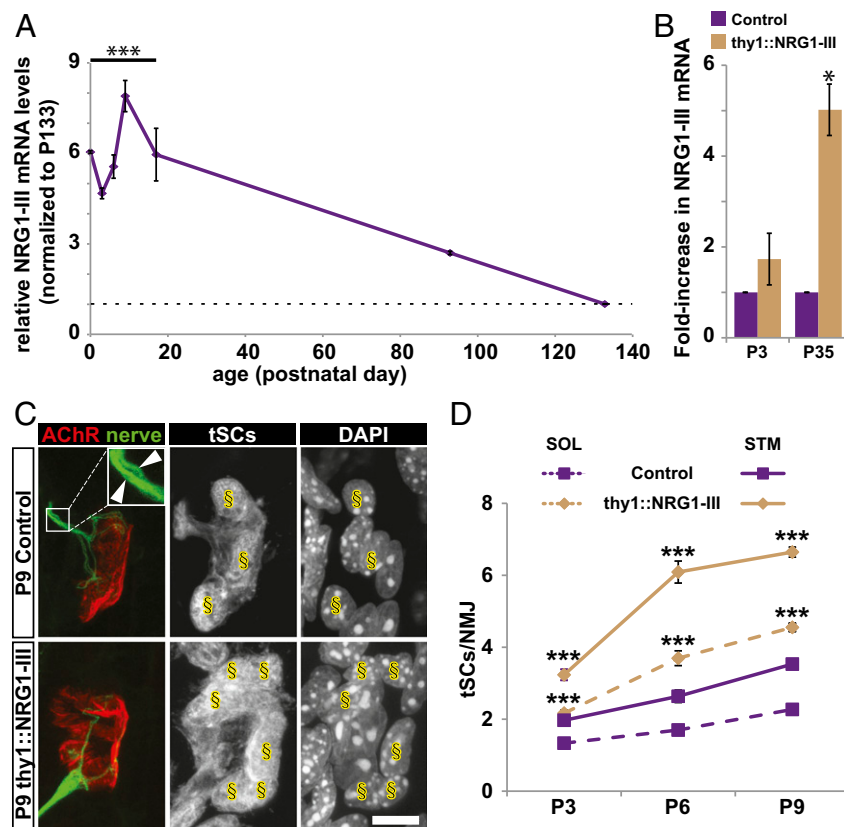


**Fig. 1.** Expression of the NRG1-III isoform in the spinal cord is developmentally regulated, and its overexpression in motor neurons increases the number of tSCs at NMJs. (A) Levels of NRG1-III in WT mouse spinal cords. All values are given relative to P133. Expression of NRG1-III is significantly higher during development (P0, P3, P6, P9, and P17, indicated by asterisks) than in adults (P133) and peaks at P9. (B) NRG1-III overexpression in the spinal cord in thy1::NRG1-III transgenic mice. At P3 and P35, NRG1-III transcript expression was approximately twofold and fivefold higher, respectively, than in WT. (C) NMJs in P9 soleus muscles of control and NRG1-III transgenic mice. Note the increased number of tSCs (§). The control NMJ is innervated by at least two motor axons (arrowheads); in contrast, the transgenic NMJ is singly innervated. (D) Counts of tSCs, identified by transgenic S100-eGFP expression (69) and DAPI staining at NMJs in soleus and sternomastoid muscles at various postnatal stages for both genotypes. (Scale bar: 10 μm.)

well-known SC mitogen (38), a twofold increase in the numbes of tSCs at NMJs (Fig. 1 C and D) is evidence of SC activation. Additional evidence of SC activation in these transgenics is provided below.

We then looked for altered rates of synapse elimination in NRG1-III–overexpressing neonates through both anatomic and physiological means. First, we immunostained for axons and determined the proportion of muscle fibers in which two or more axons entered the NMJs in sternomastoid and soleus muscles (Fig. 2A). In sternomastoid muscles, a significantly smaller fraction of NMJs in NRG1-III transgenic mice received multiple inputs at P3 (transgenic vs. control: $87.9 \pm 1.8\%$ vs. $96.0 \pm 1.0\%$; $n = 3$, $\geq 33$ NMJs per animal; $P < 0.05$) and P6 (transgenic vs. control: $44.4 \pm 2.7\%$ vs. $71.6 \pm 3.5\%$; $n = 3$, $\geq 33$ NMJs per animal; $P < 0.01$). Elimination was also accelerated in soleus by P9 (transgenic vs. control: $54.1 \pm 2.7\%$ vs. $33.3 \pm 1.9\%$; $n \geq 4$, $\geq 50$ NMJs per animal; $P < 0.001$). Endplate potentials, evoked by grading the intensity of stimuli applied to the soleus nerve (9), were also recorded from P9 soleus muscle fibers. These recordings confirmed the precocious loss of polyneuronal innervation in NRG1-III transgenic pups (transgenic vs. control: $11.7 \pm 6.0\%$ vs. $55.0 \pm 3.7\%$; $n \geq 3$, 20 fibers per animal; $P < 0.001$; Fig. 2B). Thus, increased axonal NRG1-III accelerated the loss of polyneuronal innervation at developing NMJs.

We also tested whether attenuation of axo-glial NRG1-III signaling delays synapse elimination. We examined *Nrg1* null heterozygotes that have decreased NRG1-III in peripheral nerves (25) and pups null for the beta-site APP-cleaving enzyme-1 (BACE1) (39). BACE1 is one of the enzymes that proteolytically convert NRG1 isoforms from proproteins to active fragments, and its absence reduces axo-glial NRG1-III signaling (40, 41). Significantly greater fractions of P9 soleus NMJs were polyneuronally innervated in both $NRG1^{+/-}$ mice (control vs. $NRG1^{+/-}$: $61.5 \pm 4.5\%$ vs. $77.5 \pm 4.6\%$; $n = 4$; $P < 0.05$,; Fig. S1) and $BACE1^{-/-}$ mice (control vs. $BACE1^{-/-}$: $55.0 \pm 3.7\%$ vs. $85.0 \pm 5.0\%$; $n \geq 3$, 20 NMJs per animal; $P < 0.01$; Fig. 2B). Consistent with decreased NRG1-III signaling, we found fewer tSCS at NMJs of NRG1 heterozygotes (control vs. $NRG1^{+/-}$: $3.2 \pm 0.1\%$ vs. $2.2 \pm 0.1\%$; $n = 4$; $P < 0.001$, Fig. S1). Thus, these findings argue strongly that the strength of axo-glial NRG1-III signaling, as indicated by changes in the number of tSCs at the synapse, regulates the rate of redundant motor axon pruning at developing NMJs.

### Increased Axo-Glial NRG1-III Signaling Induces Profound Morphological Alterations of Adult Mouse NMJs.

Synapse elimination at developing rodent NMJs is normally completed by the end of the second postnatal week. Elevated expression of NRG1-III in the transgenic mice continues into adulthood (Fig. 1B). Therefore, we looked for evidence of continued synaptic remodeling in these adults. We found that postsynaptic AChR aggregates were fragmented into small "islands," a pattern distinct from control mature NMJs, whose continuous gutters of AChR resemble pretzels (Fig. 3A). In P21 sternomastoid muscles of the transgenic mice, an average of 17 separate AChR-rich islands were present at each NMJ, compared with fewer than 4 in controls (Fig. 3B and Table S1). The number of islands at NRG1-III NMJs increased until P42 and remained unchanged thereafter at 24 per NMJ. In contrast, there were only seven separate AChR-rich gutters in controls at P140. The presynaptic nerve terminals were also affected by NRG1-III overexpression; terminal varicosities, in contrast to terminal branches of mostly even caliber seen at control NMJs, apposed the AChR-rich islands (Fig. 3A). These marked changes appeared at all junctions in all muscles examined, including sternomastoid, soleus, triangularis sterni, and diaphragm.

The NMJs of NRG1-III–overexpressing mice resembled those seen in aged or dystrophic mice, whose fragmented AChR morphology and varicose nerve terminals appear to be due to necrosis of synaptic myofiber segments and their ensuing regeneration (4, 42, 43). We found no change in the number of centrally nucleated fibers in muscles of transgenics, however (Fig. S2; 2.49% and 6.85% in two controls vs. 4.01% and 5.53% in two transgenic littermates), which argues against their degeneration and regeneration. Another potential cause of fragmentation is a perturbation of agrin/MuSK signaling (44, 45); however, immunostaining showed that agrin remained concentrated at the NMJs of NRG1-III transgenic mice, and that phosphorylation of AChR β subunit—an event closely coupled with agrin-induced AChR clustering (46, 47)—was observed throughout AChR aggregates (Fig. S2). In addition, we failed to observe denervated NMJs in transgenic animals. Thus, the mechanism of fragmentation of NRG1-III transgenic junctions appears to be different from the fragmentation in aging and dystrophy.

Despite the presynaptic and postsynaptic changes, tSC coverage of the synapses was retained in the adult transgenic mice (Fig. 3). Nonetheless, tSCs did respond to increased NRG1-III expression. There was a twofold increase in the number of tSCs at transgenic NMJs (Fig. 3C) that preceded any obvious alterations to the synapse (see the vital imaging data below). As with the numbers of AChR-rich islands, the number of tSCs remained subsequently unchanged in adult control and transgenic mice
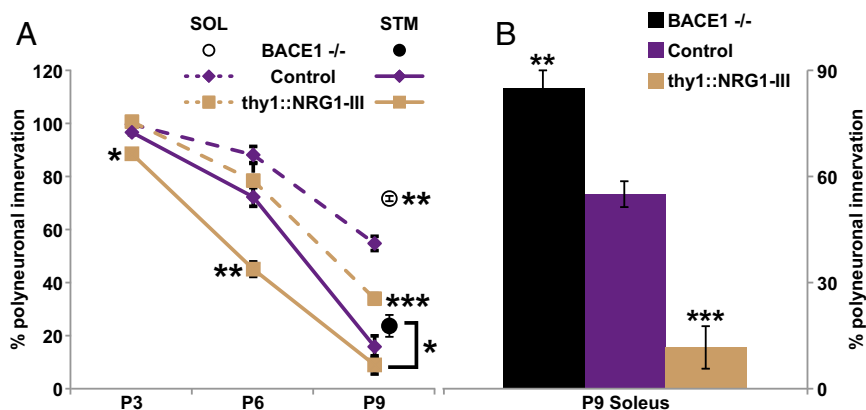


**Fig. 2.** Level of NRG1-III signaling correlates with the rate of developmental synapse elimination at NMJs. (A) Fraction of NMJs in NRG1-III–overexpressing animals and their control littermates that were polyneuronally innervated, determined at P3, P6, and P9 by immunostaining the axons entering individual NMJs (as in Fig. 1B). Synapse elimination is accelerated by increased expression of neuronal NRG1-III (gold lines). Conversely, the rate of synapse elimination is slowed in BACE1$^{-/-}$, where NRG1-III processing is impaired. Synapse elimination occurs earlier in sternomastoid (solid lines) than in soleus (dashed lines), because of an anterior-posterior developmental gradient (70, 72). (B) Determination of innervation status through intracellular recordings of endplate potentials yielded similar results.
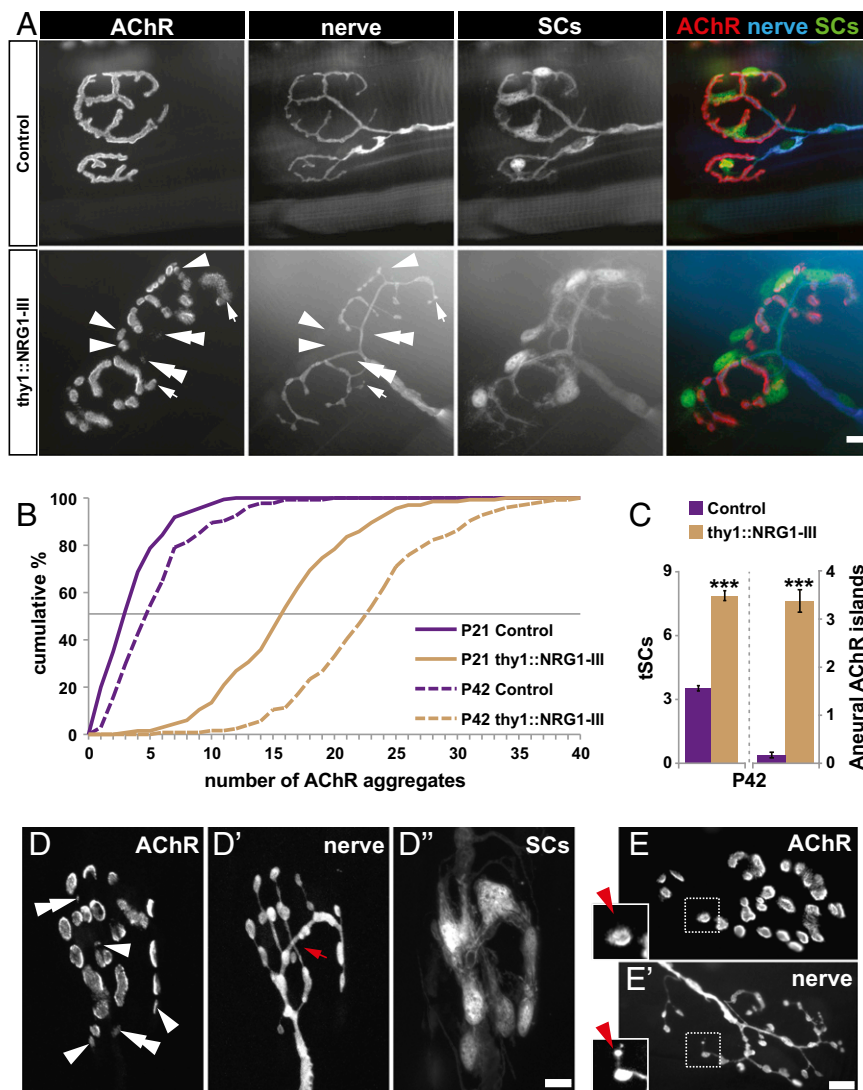
**Fig. 3.** NRG1-III overexpression remodels adult NMJs. (*A*) AChR, tSCs, and nerve terminals are altered in response to NRG1-III overexpression. AChR aggregates in controls appear "pretzel-like," but are "fragmented" into AChR-rich "islands" in transgenics. Motor axon terminals, visualized by thy1-driven CFP expression (67), appear varicose compared with those of controls where branches are of even caliber. Some AChR-rich islands are aneural (arrowheads; also see Fig. 3*D*). Dim labeling of AChR (double arrowheads) indicates aneural islands that contain fewer receptors and would be expected to be lost eventually (19). Varicose terminal branches over still-contiguous AChR gutters (arrows) suggest that presynaptic remodeling precedes postsynaptic remodeling. (*B*) Fragmentation of AChR is apparent in the increased number of AChR-rich islands at P21 (solid lines) and a further increase after an additional 3 wk (P42; dashed lines). (*C*) A sustained increase in axo-glial NRG1-III signaling results in more than a doubling of tSC numbers and occurrence of aneural AChR-rich islands at adult NMJs (also see Table S1). (*D*) Some transgenic NMJs show terminal branches of the motor axon crossing each other to innervate the muscle (*D'*, red arrow). (*E*) Intrajunctional terminal sprouts occur at NRG1-III transgenic NMJs. (*Insets*) Higher-magnification images of the sprouting event (red arrowhead). (Scale bars: 10 μm.)

alike (Table S1). tSCs of transgenic NMJs also extended numerous processes to areas between synaptic gutters (Fig. 3), a feature absent at normal, mature junctions, suggesting activation of these cells. Consistent with the idea that the postnatal peak in NRG1-III expression is responsible for the behaviors of neonatal tSCs and subsequent synaptic changes, overexpression of NRG1-III in adults imposes neonate-like features on tSCs and results in presynaptic and postsynaptic alterations.

A partial rescue of these morphological deviations was achieved when the NRG1-III–overexpressing mice also lacked BACE1 (thy1::NRG1-III; BACE1$^{-/-}$) (Fig. S3). Here the effects of NRG1-III overexpression would be expected to be attenuated through reduced processing. Thy1::NRG1-III; BACE1$^{-/-}$ NMJs had significantly fewer AChR-rich islands (11.18 ± 0.51) compared with NRG1-III transgenic animals (19.15 ± 0.7), but more

than controls (5.58 ± 0.28; $n \geq 3$; $P < 0.001$). The same was true for the number of tSCs (double mutants vs. NRG1-III transgenics vs. controls: 7.31 ± 0.24 vs. 5.56 ± 0.14 vs. 3.37 ± 0.10; $n \geq 3$; $P < 0.001$). The incomplete rescue is consistent with BACE1 not being the sole enzyme responsible for NRG1-III processing (36). In addition, NMJs of mice overexpressing NRG1 type I (instead of type III) under the same thy1.2 promoter remained unaltered (Fig. S3). Thus, the changes that we observed at adult NMJs require a sustained increase in NRG1-III tethered to motor axonal membranes and its augmentation of axo-SC signaling.

**Alterations of NMJ Morphology Are Concurrent with Dynamism of Synaptic Components.** Major morphological alterations at normal rodent NMJs, other than in aging or disease, are restricted to the
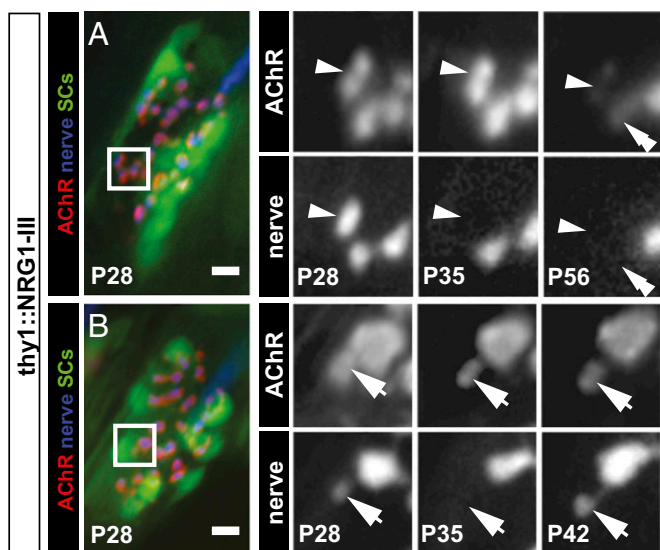
**Fig. 4.** Fates of aneural portions of postsynaptic AChR in NRG1-III transgenic mice. NMJs of NRG1-III transgenic mice were vitally imaged beginning at P28. Boxed portions of the endplates at different ages are shown to the right at higher magnification. (*A*) An AChR-rich island at the end of a terminal branch (arrowhead) becomes aneural during the first week and is eliminated from the muscle membrane after another 3 wk. Between P35 and P56, another AChR-rich island (double arrowhead) becomes aneural. (*B*) A presynaptic bouton withdraws from an AChR-rich island (arrow) during the first week of imaging and returns to innervate this AChR aggregate during the second week. (Scale bars: 10 μm.)

first 3 wk of postnatal life, roughly coincident with the period of synapse elimination (8, 12). Our results reported here support our hypothesis that synaptic remodeling seen at NMJs of NRG1-III

transgenic mice results from neonate-like plasticity of its components associated with tSC activation.

First, and most obvious, we found aneural AChR-rich islands (Fig. 3, arrowheads). At P21, an average of five such postsynaptic islands without a presynaptic nerve branch were present at NRG1-III transgenic NMJs (Table S2). These aneural AChR-rich islands likely result from pruning of presynaptic terminal branches, as demonstrated by the vital imaging findings presented below. Recent studies strongly argue that such branch pruning occurs at developing NMJs and drives synapse elimination (11, 16).

Aneural and thus inactive AChR clusters within an active NMJ would be expected to be removed from the muscle membrane (19). Indeed, an average of two of the five abandoned AChR islands per junction have diminished AChR density compared with those still innervated (Fig. 3, double arrowheads, and Table S2), suggesting that they eventually will be lost completely. Additional support for the idea that abandoned AChR islands are eventually eliminated from the postsynaptic membrane comes from the presence of acetylcholine esterase (AChE) over sites that lack both AChR and nerve apposition (Fig. S4). Given that components of synaptic basal lamina turn over more slowly than postsynaptic AChR (48), such AChE labeling likely indicates sites of recent AChR loss. The strongest evidence, however, comes from repeated vital imaging of NMJs in NRG1-III transgenic mice showing that abandoned AChR-rich islands disappear with time (Fig. 4*A*). In such cases, the rate of AChR removal from postsynaptic membrane was consistent with that observed at normal NMJs (19). These abandoned AChR aggregates are found along the course, as well as at the tips, of nerve terminal branches, and thus are not likely the result solely of extension/retraction of motor nerve terminals.

If portions of the synapse are continuously removed, then denervation of NMJs may result. Past P42, however, the average number of AChR-rich islands at NMJs of NRG1-III–overexpressing
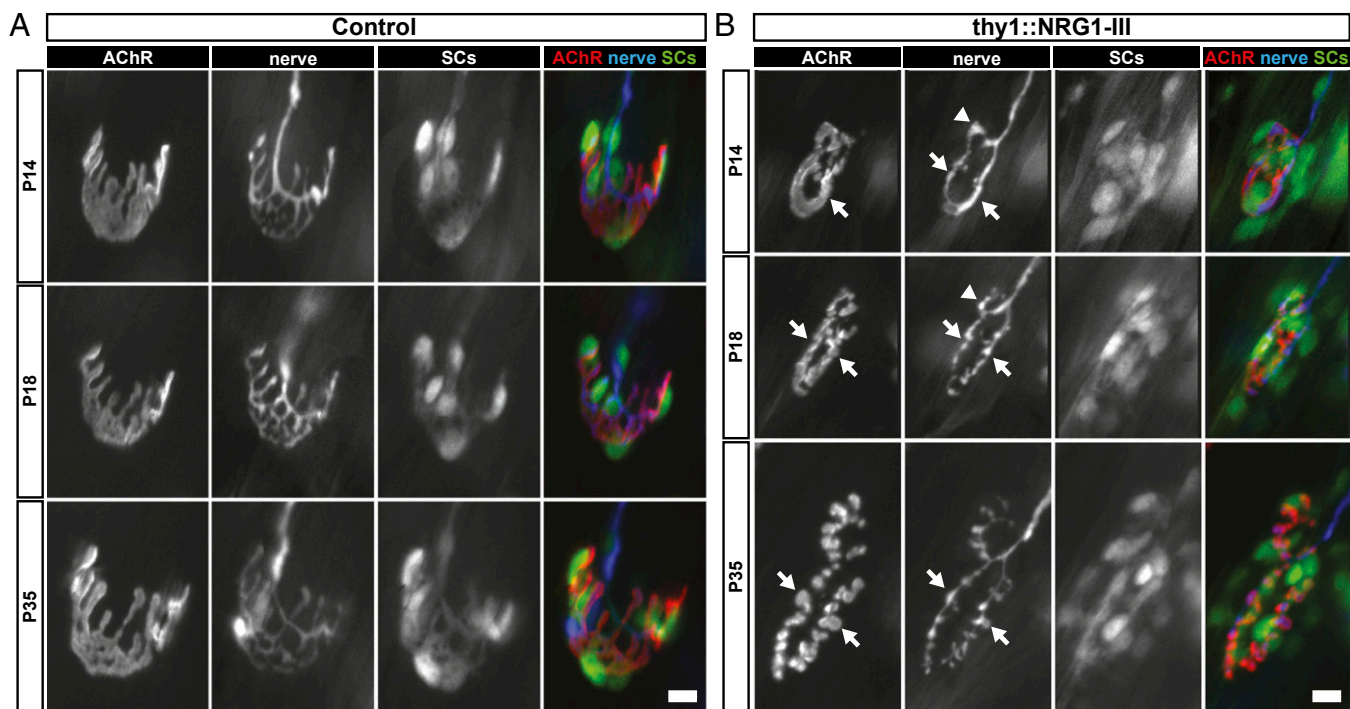


**Fig. 5.** Vital imaging shows progressive fragmentation of NRG1-III NMJs. (*A*) Control NMJ is stable over the period P14–P35. (*B*) In contrast, NMJs of NRG1-III overexpressing mice start simple at P14, but the smooth gutters of AChR fragment into islands by P35. The nerve terminals acquire varicose swellings, each of which is associated with an island. Motor axon terminals appear to alter their branch pattern at some endplates (arrowhead), and presynaptic changes precede postsynaptic changes (arrows). The images were prepared as described in the *SI Materials and Methods*. (Scale bars: 10 μm.)

mice remained stable at 24, likely due to an "offsetting" set of changes, including continued fragmentation and turnover of postsynaptic apparatus, as well as intrajunctional sprouts of presynaptic terminals (see below).

Vital imaging of the transgenic NMJs revealed that terminal branches reoccupied some aneural AChR islands (Fig. 4B). NRG1-III transgenic NMJs also had an increased frequency of terminal branches that cross over each other, with each making synaptic contact with the postsynaptic muscle fiber before and after crossing (Fig. 3D, red arrow). This crossing likely results from innervation of abandoned AChR-rich islands by intrajunctional nerve sprouts from branches distinct from the those that vacated the aggregates. There was a twofold increase in such crossings within NRG1-III transgenic NMJs (control vs. NRG1-III transgenic: $0.12 \pm 0.04$ vs. $0.26 \pm 0.05$ per NMJ; $P < 0.05$). Reoccupation of abandoned postsynaptic sites at developing NMJs also has been observed (11, 12), and this is a likely mechanism by which an axon gains advantage over its competitors during synapse elimination. Nerve sprouts (e.g., Fig. 3E) also may induce AChR aggregates de novo. Consistent with this possibility, a larger fraction of NMJs with intrajunctional nerve sprouts did not contact AChR aggregates ($0.10 \pm 0.02$ vs. $0.17 \pm 0.02$ per NMJ; $P < 0.05$) in the NRG1-III–overexpressing mice. The evidence of presynaptic changes present at sites of still-contiguous AChR-rich gutters (Fig. 3A, arrows) suggests that continuous AChR-rich gutters fragment to increase the number of AChR-rich islands.

Our observations of the NRG1-III transgenic NMJs and their ongoing morphological change (Tables S1 and S2) indicate that axonally presented NRG1-III promotes neonate-like plasticity of adult NMJs. Although this heightened dynamism appears to result in some instability of the synaptic connection, it also appears that there are mechanisms by which the synapse can grow and compensate for any loss of synaptic area. These mechanisms include fragmentation of still-contiguous AChR-rich gutters, reoc-cupation of abandoned postsynaptic portions by the nerve, and de novo AChR aggregate formation after intrajunctional nerve sprouts.

**Presynaptic Alterations Precede Postsynaptic Modifications.** At age 3 wk, NMJs in NRG1-III transgenic mice were already fragmented. Repeated vital imaging of NMJs, beginning at P14, demonstrated the transformation of what appear to be normal NMJs in NRG1-III transgenic mice. One such transformation is shown in Fig. 5. An increased number of tSCs compared with littermate control NMJs was evident at P14, before any apparent presynaptic or postsynaptic irregularities (Fig. 5B, P14), suggesting that SC responses to excess axonal NRG1-III precede other cellular events. Over the subsequent 3 wk, the morphology of transgenic NMJs was dramatically modified. Notably, by P18, before obvious postsynaptic changes, varicosities formed along the presynaptic terminal branches. A change in branching pattern was obvious as well. In contrast, control NMJs failed to show any significant changes, except for their increasing size as expected from growth of muscle fibers (49).

**Ultrastructural Examination Suggests tSC-Mediated Remodeling of the Presynaptic and Postsynaptic Apparatus.** Although the cellular events that modify adult NMJs in NRG1-III transgenic animals remain unclear, EM evidence of tSC activities likely involved in synaptic remodeling has been reported (16). Consistent with the idea that they modify the synapse, tSCs appeared to be the most dynamic cellular component at transgenic NMJs; tSCs were increased in number and also shifted the locations of their somata within the synapse (Fig. 5), unlike those at control junctions. Therefore, we examined the ultrastructure of NRG1-III transgenic NMJs. We chose to examine P16 NMJs for two reasons: (i) tSC/muscle apposition is greatly reduced by P16 at normal NMJs to the edges of nerve terminals (16), and (ii) in light microscopy, the most dramatic alterations to NMJ morphology in NRG1-III transgenic mice occur shortly after P14 (Fig. 5). Single cross-sections of NMJs as well as serial sections were examined
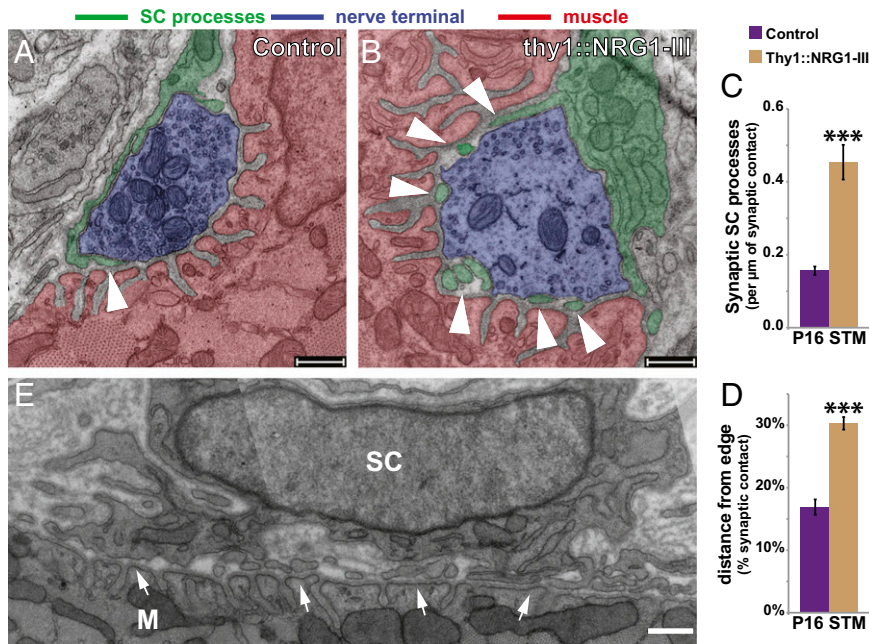


**Fig. 6.** Evidence of tSC-mediated remodeling of synaptic structures at NRG1-III NMJs. (A and B) The ultrastructure of NMJs reveals SC processes (shaded green, arrowheads) between the presynaptic nerve terminal (blue) and postsynaptic muscle membrane (red). (C) At P16, such SC intrusions into the synaptic cleft are approximately threefold more frequent than in littermate controls. (D) In addition, the intruding SC processes traverse further into the synapse. (E) tSC processes show affinity for portions of the postsynaptic membrane abandoned by nerve terminals (arrows) in this NMJ from a P40 NRG1-III sternomastoid. SCs commonly approach to within 50 nm of the muscle membrane. The secondary folds indicate this had been a site of synaptic contact. M, muscle; SC, Schwann cell soma. The images were prepared as described in the *SI Materials and Methods*. (Scale bars: 500 nm.)

at P16. tSC processes were present in the synaptic cleft at three times the frequency in control NMJs (Fig. 6 A–C and Fig. S5). These processes can be followed through consecutive serial sections and connected to tSCs above the NMJ.

The tSC processes in the overexpressing animals extended deeper into the cleft than those of control SCs and were frequently found over junctional folds, where they may interfere with chemical transmission (Fig. 6 B and D). tSCs contacted the AChR-rich surface despite the presence of laminin-β2 (Fig. S4), which has been previously reported to repel tSCs (50, 51). Such SC/muscle appositions were seen even over secondary folds of adult NMJs abandoned by the nerve (Fig. 6E and Fig. S4). Thus, as with neonates (Fig. S4) (16), tSCs are able to ignore repulsive signals and come into close contact with AChR-rich regions in response to increased axonal NRG1-III.

tSCs at NRG1-III NMJs also exhibited increased phagocytic activity directed at the presynaptic nerve terminals. Light microscopy and ultrastructural examination of NRG1-III transgenic NMJs revealed signs of such destructive SC behavior. At many of the NRG1-III transgenic NMJs, punctae of the synaptic vesicle marker synaptophysin (SP) were found outside the terminal branches outlined by transgenic CFP fluorescence (Fig. S6). These punctae appeared to be fully contained within the tSC cytoplasm. Serial EM-aided 3D reconstruction (Fig. S7) confirmed the consumption of axonal material by tSCs. Serial sections of two P16 NMJs from NRG1-III transgenic mice showed an eightfold increase in the volume of membrane debris—an indicator of phagocytic activity—over that in two control junctions (0.04 and 0.06 $\mu m^3/\mu m^2$ vs. 0.007 and 0.006 $\mu m^3/\mu m^2$ in controls).

These results resemble those seen during the period of synapse elimination and suggest a mechanism for the observed synaptic remodeling. The presynaptic nerve terminal branches are consumed and reshaped by the glial cells' phagocytic activity, in much the same way as retraction bulbs of retreating axons (52) and synaptic boutons (16) during developmental synapse elimination. Some postsynaptic AChRs are likely rendered inactive, owing to the loss of a portion of the presynaptic nerve terminal or to tSC intrusion into the synaptic cleft. Inactive AChRs like these would be expected to be lost.

## Discussion

The peak of NRG1-III expression coincides with the period of synapse elimination, and manipulations of NRG1-III signaling alter the rate of synapse elimination at developing NMJs. Moreover, normally stable adult NMJs continue to undergo modification when a high level of NRG1-III is maintained into adulthood. Thus, NRG1-III is a molecular determinant of neuromuscular synaptic plasticity (Fig. 7). We attribute these effects to tSCs on the basis of following observations. tSCs exposed to high levels of NRG1-III exhibit behaviors normally restricted to early postnatal development, including intrusion into the synaptic cleft and phagocytosis of nerve terminals. Thus, these tSC activities are not merely a consequence of competition among converging axons. Although molecular changes that underlie their synapse-modifying behaviors require further investigation, tSCs display obvious signs of NRG1-III–induced activation: they extend processes, change the position of their somata, and dramatically increase in number, likely by mitosis. Axonal NRG1-III is required to prevent tSC apoptosis during early postnatal development (53, 54), and expression of a constitutively active NRG1 receptor in tSCs results in their activation (55). Thus, tSCs are primary targets of axonal NRG1-III.

Although it is possible for motor neuron-derived-NRG1-III to affect the muscle fibers directly, this would require the membrane-anchored NRG1-III to span the width of the synaptic cleft to activate receptors on the muscle fibers. This is unlikely, especially considering that secreted, rather than transmembrane, agrin is required for synaptogenic actions on muscle fibers; NRG1-III is a smaller molecule than agrin. Proteolytic release of NRG1-III (56) would allow activation of muscle NRG1 receptors. However, NMJs of mice whose motor neurons overexpress soluble NRG1 (Fig. S3) and whose muscles lack NRG1 receptors (32) appear normal. Thus, transsynaptic NRG1-III signaling at NMJ is unlikely to contribute to synaptic remodeling. Unfortunately, at present it is infeasible to directly examine the tSC requirement for neuromuscular synapse elimination; deletion of NRG1 or receptors in SCs results in SC death and subsequent loss of muscle innervation (31, 57).

Although inducible expression of constitutively active erbB2 in neonatal SCs (55) would seem to provide another test of the role of activated tSCs in synapse elimination, tSC activation would occur without nerve contact. This might apply in the case of tSC exposure to soluble NRG1 as well. We found that soluble NRG1-I
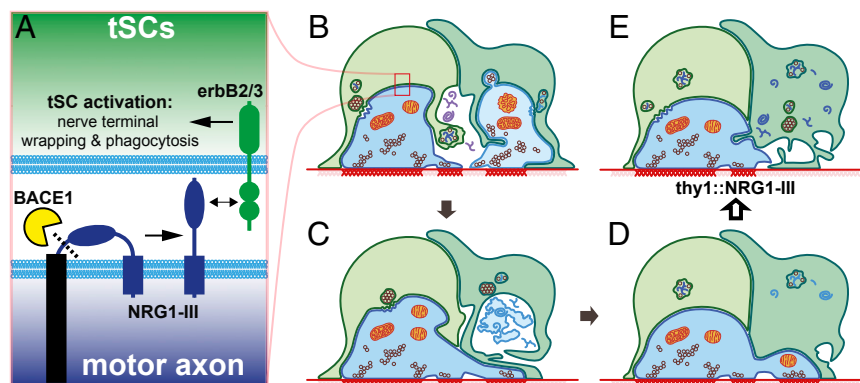


**Fig. 7.** Motor axon-tSC NRG1-III signaling regulates synapse-pruning activities of tSCs at developing NMJs. (A) Motor axons (shades of blue) present NRG1-III to erbB2/3 receptors on the surface of tSCs (shades of green) after BACE1-mediated proteolytic maturation of the NRG1-III proprotein (adapted from ref. 23). Shown is a small segment of the nerve–SC contact illustrated in B. (B and C) tSCs engage in two motor input pruning activities regulated by NRG1-III: they compete with the nerve for postsynaptic contact, and consume via phagocytosis nerve terminals. Concurrently, postsynaptic AChRs are eliminated from portions of the muscle membrane left vacant or occupied by tSCs and no longer receiving neurotransmission. Some recently abandoned postsynaptic sites are occupied on a stochastic basis by sprouts of nearby nerve terminals, and the process continues until a single motor input remains (11). (D) Synapse-altering behaviors of tSCs are down-regulated in normal adults. (E) However, in animals that overexpress NRG1-III in motor neurons (clear arrow), tSCs continue to engage in synapse-altering behavior well into adulthood, even after synapse elimination is completed.

overexpressed in motor neurons did not phenocopy the results of NRG1-III overexpression. This result is consistent with previous findings that soluble and membrane-bound NRG1 isoforms produce different responses in SCs (58). We believe that our results, taken together with previous observations, provide clear evidence for tSC activities involved in synapse elimination.

Our results add to the knowledge of roles of NRG1 in peripheral nerves. During axon outgrowth, SCs intercalate between bundles of naked axons, separating and wrapping them (21). The level of axon-to-SC NRG1-III signaling appears to determine the extent of these wrappings (as well as the ratio of SCs to axons) (25, 26). NRG1 is also responsible for aspects of SC activities in injured nerves. Following axotomy in the adult, an increase in autocrine NRG1 signaling is associated with degeneration of axons, as SCs up-regulate their expression of both NRG1 and its receptors (59). Interestingly, tSCs at NMJs after nerve injury exhibit many of the behaviors reported in these same cells during development, intruding into the synaptic cleft and consuming portions of nerve terminals (60, 61). Thus, NRG1 appears to influence the activities of SCs throughout life.

### Activity-Dependent Regulation of Axo-Glial NRG1 Signaling.
Neuromuscular activity is a critical factor in neuromuscular synapse elimination (14, 15). Our observations are completely compatible with the roles of such activity. First, neuromuscular activity could regulate the strength of axo-glial NRG1-III signaling. Increased activity has been found to promote the transcription of NRG1-III by rat cortical neurons in vitro (35). Given that most NRG1 isoforms are produced initially as an inactive proprotein and then undergo proteolytic maturation (23), the processing itself could be activity-dependent (62). Synapse elimination is delayed in the absence of BACE1, and thus proteolytic maturation of NRG1-III by BACE1 (and other proteases) also presents a possible point of activity-dependent regulation. Both nerve- and SC-derived BACE1 appear capable of NRG1 processing (63); however, the source of BACE1 that presumably regulates tSC behavior is unclear. Thus, our results are consistent with a model in which axonal NRG1-III, on activity-driven proteolytic conversion, provides tSCs with a stimulus to engage in behaviors that promote synaptic remodeling. Considering that expression of NRG1-III peaks early in life and declines into adulthood, this model also helps explain the remarkable morphological stability of adult NMJs.

### Comparisons with Other Cases of Synapse Elimination.
In both central and peripheral nervous systems, synapse elimination is experience-driven and demonstrates glial participation. Specifically, in the mouse visual system, both astrocytes and microglia within the lateral geniculate nucleus phagocytose and degrade synaptic inputs of retinal ganglion cells (64, 65). This process relies in part on expression of the complement cascade system. How activity differentially targets synapses for glial consumption is unknown; however, subclasses of major histocompatibility complex 1 molecules appear to be involved in determining the specificity of synaptic pruning (66).

## Materials and Methods

**Animals.** Experiments were conducted in accordance with National Institutes of Health guidelines and were approved by the Institutional Animal Care and Use Committees at The University of Texas and Texas A&M University. The generation of transgenic and mutant mice has been described previously (25, 39, 67–69).

**Fluorescent Immunostaining.** NMJs were labeled in whole mounts as described previously (43, 70). Fluorophore-conjugated fasciculin-2 was prepared as described previously (71). Neonatal motor axons were labeled with anti-neurofilament (2H3; Developmental Studies Hybridoma Bank). DAPI was used in combination with GFP labeling to mark and count SCs. Images were acquired with a Leica DMR epifluorescence microscope equipped with a Hamamatsu cooled CCD camera or a Leica TCS SP5 confocal system.

**EM.** Muscle preparation for EM, image acquisition, and analysis were performed as described previously (16).

**qRT-PCR.** Spinal cords were dissected from WT and NRG1-III–overexpressing mice. Total RNA was isolated from each spinal cord using TRIzol reagent (Invitrogen), and its purity and integrity was assayed using the RNA 6000 Nano Kit (Agilent Technologies). Samples were reverse-transcribed, and qRT-PCR was performed in quadruplicate on a ViiA 7 Real-Time PCR system. Expression of NRG1-III in each sample group was normalized to 18S levels.

**Physiology.** Polyneuronal innervation was examined by intracellular recordings of P9 soleus muscle fibers as described previously (14).

**Statistical Analysis.** Statistical analysis (one-way ANOVA with Bonferroni post hoc or Student's $t$ test) of raw data and the generation of histograms were performed using GraphPad Prism software and Microsoft Excel spreadsheet software. $*P < 0.05$; $**P < 0.01$; $***P < 0.001$. Numerical data are reported as mean $\pm$ SEM.

1. Yu X, et al. (2013) Accelerated experience-dependent pruning of cortical synapses in ephrin-A2 knockout mice. *Neuron* 80(1):64–71.
2. Nishiyama N, Colonna J, Shen E, Carrillo J, Nishiyama H (2014) Long-term in vivo time-lapse imaging of synapse development and plasticity in the cerebellum. *J Neurophysiol* 111(1):208–216.
3. Fu M, Yu X, Lu J, Zuo Y (2012) Repetitive motor learning induces coordinated formation of clustered dendritic spines in vivo. *Nature* 483(7387):92–95.
4. Lyons PR, Slater CR (1991) Structure and function of the neuromuscular junction in young adult mdx mice. *J Neurocytol* 20(12):969–981.
5. Balice-Gordon RJ (1997) Age-related changes in neuromuscular innervation. *Muscle Nerve Suppl* 5:S83–S87.
6. Robitaille R (1998) Modulation of synaptic efficacy and synaptic depression by glial cells at the frog neuromuscular junction. *Neuron* 21(4):847–855.
7. Jahromi BS, Robitaille R, Charlton MP (1992) Transmitter release increases intracellular calcium in perisynaptic Schwann cells in situ. *Neuron* 8(6):1069–1077.
8. Balice-Gordon RJ, Lichtman JW (1993) In vivo observations of pre- and postsynaptic changes during the transition from multiple to single innervation at developing neuromuscular junctions. *J Neurosci* 13(2):834–855.
9. Brown MC, Jansen JK, Van Essen D (1976) Polyneuronal innervation of skeletal muscle in new-born rats and its elimination during maturation. *J Physiol* 261(2):387–422.
10. Tapia JC, et al. (2012) Pervasive synaptic branch removal in the mammalian neuromuscular system at birth. *Neuron* 74(5):816–829.
11. Turney SG, Lichtman JW (2012) Reversing the outcome of synapse elimination at developing neuromuscular junctions in vivo: Evidence for synaptic competition and its mechanism. *PLoS Biol* 10(6):e1001352.
12. Walsh MK, Lichtman JW (2003) In vivo time-lapse imaging of synaptic takeover associated with naturally occurring synapse elimination. *Neuron* 37(1):67–73.
13. Personius KE, Chang Q, Mentis GZ, O'Donovan MJ, Balice-Gordon RJ (2007) Reduced gap junctional coupling leads to uncorrelated motor neuron firing and precocious neuromuscular synapse elimination. *Proc Natl Acad Sci USA* 104(28):11808–11813.
14. Thompson W (1983) Synapse elimination in neonatal rat muscle is sensitive to pattern of muscle use. *Nature* 302(5909):614–616.
15. Buffelli M, et al. (2003) Genetic evidence that relative synaptic efficacy biases the outcome of synaptic competition. *Nature* 424(6947):430–434.
16. Smith IW, Mikesh M, Lee Yi, Thompson WJ (2013) Terminal Schwann cells participate in the competition underlying neuromuscular synapse elimination. *J Neurosci* 33(45):17724–17736.
17. Marques MJ, Conchello JA, Lichtman JW (2000) From plaque to pretzel: Fold formation and acetylcholine receptor loss at the developing neuromuscular junction. *J Neurosci* 20(10):3663–3675.
18. Slater CR (1982) Postnatal maturation of nerve–muscle junctions in hindlimb muscles of the mouse. *Dev Biol* 94(1):11–22.
19. Balice-Gordon RJ, Lichtman JW (1994) Long-term synapse loss induced by focal blockade of postsynaptic receptors. *Nature* 372(6506):519–524.
20. Korneliussen H, Jansen JK (1976) Morphological aspects of the elimination of polyneuronal innervation of skeletal muscle fibres in newborn rats. *J Neurocytol* 5(8):591–604.
21. Peters A, Muir AR (1959) The relationship between axons and Schwann cells during development of peripheral nerves in the rat. *Q J Exp Physiol Cogn Med Sci* 44(1):117–130.

22. Burden S, Yarden Y (1997) Neuregulins and their receptors: A versatile signaling module in organogenesis and oncogenesis. *Neuron* 18(6):847–855.

23. Falls DL (2003) Neuregulins: Functions, forms, and signaling strategies. *Exp Cell Res* 284(1):14–30.

24. Mei L, Nave KA (2014) Neuregulin-ERBB signaling in the nervous system and neuro-psychiatric diseases. *Neuron* 83(1):27–49.

25. Michailov GV, et al. (2004) Axonal neuregulin-1 regulates myelin sheath thickness. *Science* 304(5671):700–703.

26. Taveggia C, et al. (2005) Neuregulin-1 type III determines the ensheathment fate of axons. *Neuron* 47(5):681–694.

27. Yang X, Kuo Y, Devay P, Yu C, Role L (1998) A cysteine-rich isoform of neuregulin controls the level of expression of neuronal nicotinic receptor channels during syn-aptogenesis. *Neuron* 20(2):255–270.

28. Meyer D, et al. (1997) Isoform-specific expression and function of neuregulin. *Development* 124(18):3575–3586.

29. Falls DL, Rosen KM, Corfas G, Lane WS, Fischbach GD (1993) ARIA, a protein that stimulates acetylcholine receptor synthesis, is a member of the neu ligand family. *Cell* 72(5):801–815.

30. Jessell TM, Siegel RE, Fischbach GD (1979) Induction of acetylcholine receptors on cultured skeletal muscle by a factor extracted from brain and spinal cord. *Proc Natl Acad Sci USA* 76(10):5397–5401.

31. Jaworski A, Burden SJ (2006) Neuromuscular synapse formation in mice lacking motor neuron- and skeletal muscle-derived Neuregulin-1. *J Neurosci* 26(2):655–661.

32. Escher P, et al. (2005) Synapses form in skeletal muscles lacking neuregulin receptors. *Science* 308(5730):1920–1923.

33. Trachtenberg JT, Thompson WJ (1997) Nerve terminal withdrawal from rat neuromus-cular junctions induced by neuregulin and Schwann cells. *J Neurosci* 17(16):6243–6255.

34. Cohen JA, Yachnis AT, Arai M, Davis JG, Scherer SS (1992) Expression of the neu proto-oncogene by Schwann cells during peripheral nerve development and Wallerian degeneration. *J Neurosci Res* 31(4):622–634.

35. Liu X, et al. (2011) Specific regulation of NRG1 isoform expression by neuronal activity. *J Neurosci* 31(23):8491–8501.

36. Velanac V, et al. (2012) Bace1 processing of NRG1 type III produces a myelin-inducing signal but is not essential for the stimulation of myelination. *Glia* 60(2):203–217.

37. Agarwal A, et al. (2014) Dysregulated expression of neuregulin-1 by cortical pyra-midal neurons disrupts synaptic plasticity. *Cell Reports* 8(4):1130–1145.

38. Lemke GE, Brockes JP (1984) Identification and purification of glial growth factor. *J Neurosci* 4(1):75–83.

39. Cai H, et al. (2001) BACE1 is the major beta-secretase for generation of Abeta pep-tides by neurons. *Nat Neurosci* 4(3):233–234.

40. Hu X, et al. (2006) Bace1 modulates myelination in the central and peripheral nervous system. *Nat Neurosci* 9(12):1520–1525.

41. Willem M, et al. (2006) Control of peripheral nerve myelination by the beta-secretase BACE1. *Science* 314(5799):664–666.

42. Li Y, Thompson WJ (2011) Nerve terminal growth remodels neuromuscular synapses in mice following regeneration of the postsynaptic muscle fiber. *J Neurosci* 31(37):13191–13203.

43. Li Y, Lee Yi, Thompson WJ (2011) Changes in aging mouse neuromuscular junctions are explained by degeneration and regeneration of muscle fiber segments at the synapse. *J Neurosci* 31(42):14910–14919.

44. Linnoila J, Wang Y, Yao Y, Wang ZZ (2008) A mammalian homolog of *Drosophila* tumorous imaginal discs, Tid1, mediates agrin signaling at the neuromuscular junc-tion. *Neuron* 60(4):625–641.

45. Samuel MA, Valdez G, Tapia JC, Lichtman JW, Sanes JR (2012) Agrin and synaptic laminin are required to maintain adult neuromuscular junctions. *PLoS One* 7(10):e46663.

46. Ferns M, Deiner M, Hall Z (1996) Agrin-induced acetylcholine receptor clustering in mammalian muscle requires tyrosine phosphorylation. *J Cell Biol* 132(5):937–944.

47. Borges LS, et al. (2008) Identification of a motif in the acetylcholine receptor beta subunit whose phosphorylation regulates rapsyn association and postsynaptic re-ceptor localization. *J Neurosci* 28(45):11468–11476.

48. Culican SM, Nelson CC, Lichtman JW (1998) Axon withdrawal during synapse elimi-nation at the neuromuscular junction is accompanied by disassembly of the post-synaptic specialization and withdrawal of Schwann cell processes. *J Neurosci* 18(13):4953–4965.

49. Balice-Gordon RJ, Breedlove SM, Bernstein S, Lichtman JW (1990) Neuromuscular junctions shrink and expand as muscle fiber size is manipulated: In vivo observations in the androgen-sensitive bulbocavernosus muscle of mice. *J Neurosci* 10(8):2660–2671.

50. Noakes PG, Gautam M, Mudd J, Sanes JR, Merlie JP (1995) Aberrant differentiation of neuromuscular junctions in mice lacking s-laminin/laminin beta 2. *Nature* 374(6519):258–262.

51. Patton BL, Chiu AY, Sanes JR (1998) Synaptic laminin prevents glial entry into the synaptic cleft. *Nature* 393(6686):698–701.

52. Bishop DL, Misgeld T, Walsh MK, Gan WB, Lichtman JW (2004) Axon branch removal at developing synapses by axosome shedding. *Neuron* 44(4):651–661.

53. Trachtenberg JT, Thompson WJ (1996) Schwann cell apoptosis at developing neuro-muscular junctions is regulated by glial growth factor. *Nature* 379(6561):174–177.

54. Wolpowitz D, et al. (2000) Cysteine-rich domain isoforms of the neuregulin-1 gene are required for maintenance of peripheral synapses. *Neuron* 25(1):79–91.

55. Hayworth CR, et al. (2006) Induction of neuregulin signaling in mouse Schwann cells in vivo mimics responses to denervation. *J Neurosci* 26(25):6873–6884.

56. Fleck D, et al. (2013) Dual cleavage of neuregulin 1 type III by BACE1 and ADAM17 liberates its EGF-like domain and allows paracrine signaling. *J Neurosci* 33(18):7856–7869.

57. Lin W, et al. (2000) Aberrant development of motor axons and neuromuscular syn-apses in erbB2-deficient mice. *Proc Natl Acad Sci USA* 97(3):1299–1304.

58. Leimeroth R, et al. (2002) Membrane-bound neuregulin1 type III actively promotes Schwann cell differentiation of multipotent progenitor cells. *Dev Biol* 246(2):245–258.

59. Carroll SL, Miller ML, Frohnert PW, Kim SS, Corbett JA (1997) Expression of neu-regulins and their putative receptors, ErbB2 and ErbB3, is induced during Wallerian degeneration. *J Neurosci* 17(5):1642–1659.

60. Jirmanová I, Thesleff S (1972) Ultrastructural study of experimental muscle de-generation and regeneration in the adult rat. *Z Zellforsch Mikrosk Anat* 131(1):77–97.

61. Miledi R, Slater CR (1970) On the degeneration of rat neuromuscular junctions after nerve section. *J Physiol* 207(2):507–528.

62. Loeb JA, Hmadcha A, Fischbach GD, Land SJ, Zakarian VL (2002) Neuregulin expres-sion at neuromuscular synapses is modulated by synaptic activity and neurotrophic factors. *J Neurosci* 22(6):2206–2214.

63. Hu X, Hu J, Dai L, Trapp B, Yan R (2015) Axonal and Schwann cell BACE1 is equally required for remyelination of peripheral nerves. *J Neurosci* 35(9):3806–3814.

64. Chung WS, et al. (2013) Astrocytes mediate synapse elimination through MEGF10 and MERTK pathways. *Nature* 504(7480):394–400.

65. Schafer DP, et al. (2012) Microglia sculpt postnatal neural circuits in an activity and complement-dependent manner. *Neuron* 74(4):691–705.

66. Lee H, et al. (2014) Synapse elimination and learning rules co-regulated by MHC class I H2-Db. *Nature* 509(7499):195–200.

67. Feng G, et al. (2000) Imaging neuronal subsets in transgenic mice expressing multiple spectral variants of GFP. *Neuron* 28(1):41–51.

68. Meyer D, Birchmeier C (1995) Multiple essential functions of neuregulin in develop-ment. *Nature* 378(6555):386–390.

69. Zuo Y, et al. (2004) Fluorescent proteins expressed in mouse transgenic lines mark subsets of glia, neurons, macrophages, and dendritic cells for vital examination. *J Neurosci* 24(49):10999–11009.

70. Lee YI, Mikesh M, Smith I, Rimer M, Thompson W (2011) Muscles in a mouse model of spinal muscular atrophy show profound defects in neuromuscular development even in the absence of failure in neuromuscular transmission or loss of motor neurons. *Dev Biol* 356(2):432–444.

71. Lee Y, Li Y (2015) The use of synaptic basal lamina and its components to identify sites of recent morphological alterations at mammalian neuromuscular junctions. *Extracellular Matrix*, eds Leach JB, Powell EM (Springer, New York), Vol 93, pp 13–22.

72. Bixby JL, van Essen DC (1979) Regional differences in the timing of synapse elimina-tion in skeletal muscles of the neonatal rabbit. *Brain Res* 169(2):275–286.

73. Gillespie SK, Balasubramanian S, Fung ET, Huganir RL (1996) Rapsyn clusters and ac-tivates the synapse-specific receptor tyrosine kinase MuSK. *Neuron* 16(5):953–962.

74. Sugiyama J, Bowen DC, Hall ZW (1994) Dystroglycan binds nerve and muscle agrin. *Neuron* 13(1):103–115.

75. Sasaki T, Mann K, Miner JH, Miosge N, Timpl R (2002) Domain IV of mouse laminin beta1 and beta2 chains. *Eur J Biochem* 269(2):431–442.

76. Fiala JC (2005) Reconstruct: A free editor for serial section microscopy. *J Microsc* 218(Pt 1):52–61.

NEUROSCIENCE